Supplementary Figure 1 – The MICROMEK liquid handling device

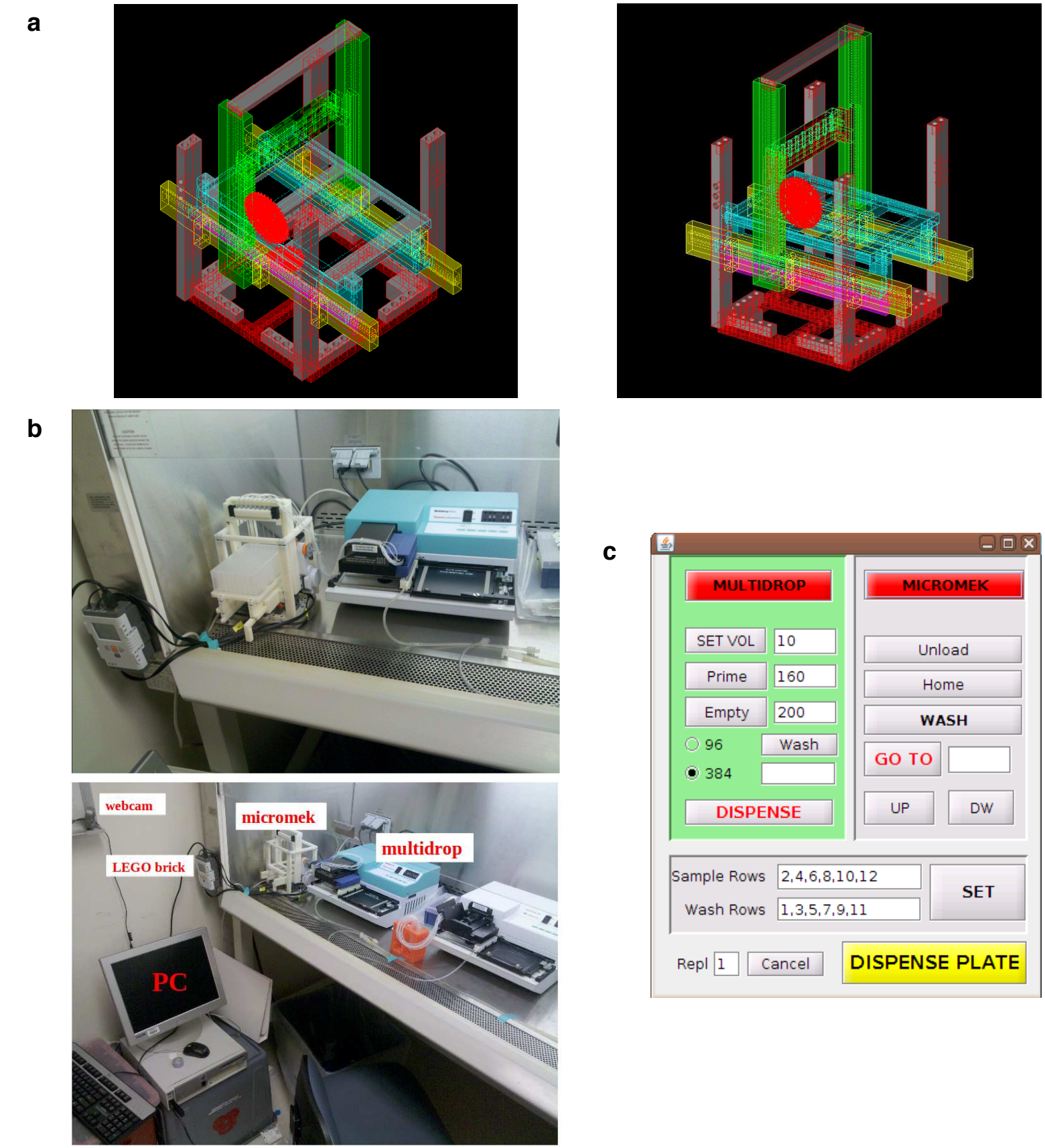

The MICROMEK liquid handling device. The instrument was built using the LEGO Mindstorms kit (http://mindstorms.lego.com) and plastic parts manufactured using a 3D printer (uPrint, http://www.uprint3dprinting.com/). Parts design was done using BRL-CAD (http://brlcad.org/). All the CAD files and scheduling software running the MICROMEK and Multidrop are available upon request. A video of the instrument in action is available at: http://www.youtube.com/watch?v=CU-dOno6FzI. (**a**) CAD drawings of MICROMEK viewed from different angles with individual parts colored. (**b**) The MICROMEK connected to a Multidrop dispenser (Thermo) in a tissue culture hood with different components annotated. The whole setup has very small footprint and is operated through a PC running custom-built scheduling software. The instruments can also be run remotely using desktop virtualization software and a webcam. (**c**) The control panel for running the MICROMEK and Multidrop from a PC. The software was developed in Java. The communication with the Multidrop is via a serial RS232 port using the standard Multidrop command set per manufacturer's documentation. The PC talks to the LEGO brick through a USB connection using a custom-built driver.

Nature Methods: doi:10.1038/nmeth.2398

Supplementary Figure 2 – Data reproducibility

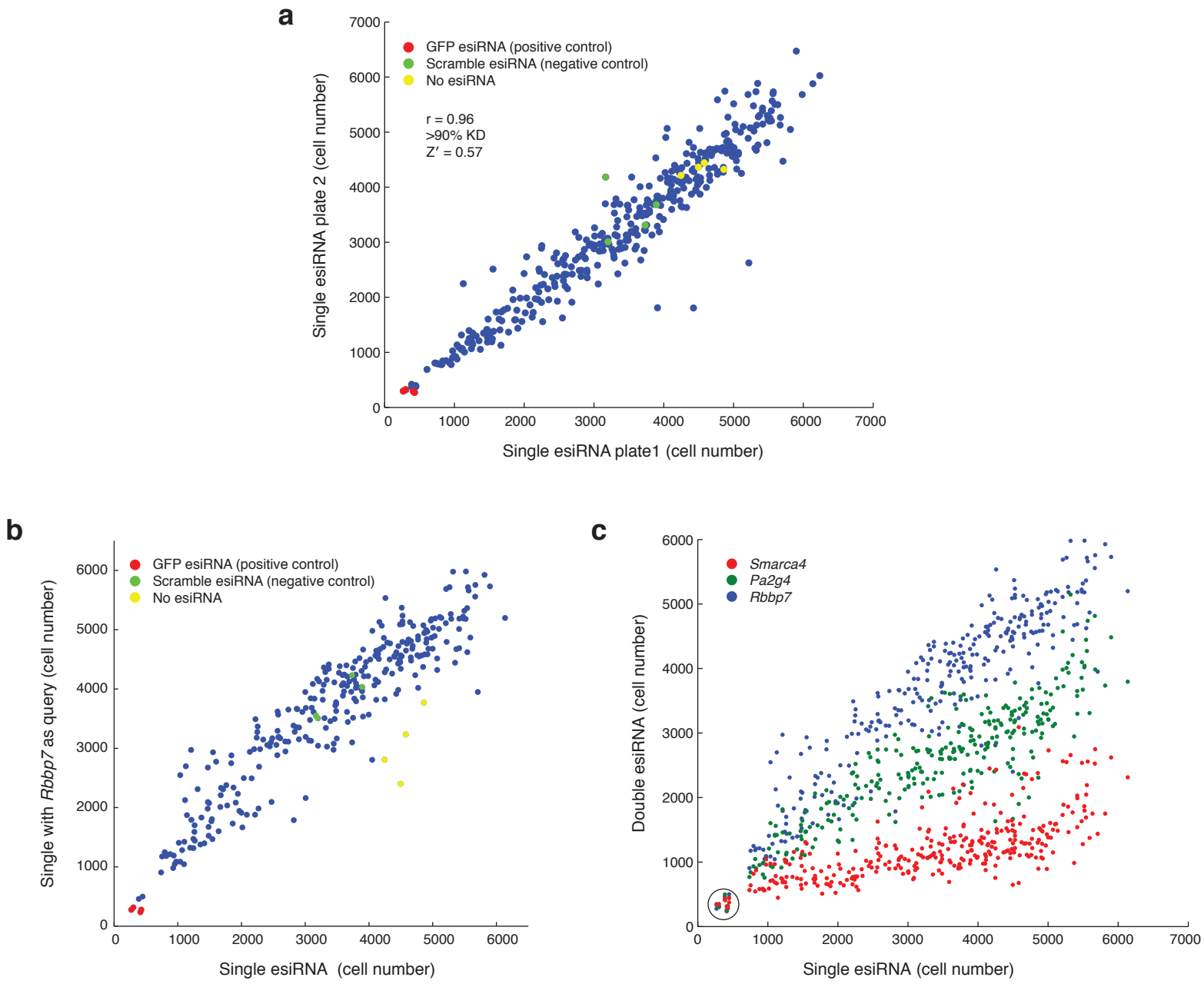

Data reproducibility. (**a**) Reproducibility of the experimental protocol. Raw data corresponding to two independent replicate single esiRNA experiments are presented with data-points for the positive control (GFP), mock-transfected and scramble control indicated. Pearson correlation, percentage difference between scramble and GFP and screening Z-factor are listed (**b**) The addition of a second esiRNA causes a mild effect consistent with the assumptions used for deriving the GIs scores (*S-scores*). (**c**) Fitness defects associated with a particular gene knockdown are easily observable upon combination with second esiRNAs. Raw data for three query genes (Smarca4, Pa2g4 and Rbbp7) is shown. Each point represents the combination of a query with another gene knockdown, for a total of 384 per query. Data points corresponding to GFP positive controls are circled. For all three panels raw cell numbers are used.

Supplementary Figure 3 – Comparison of GI scoring systems

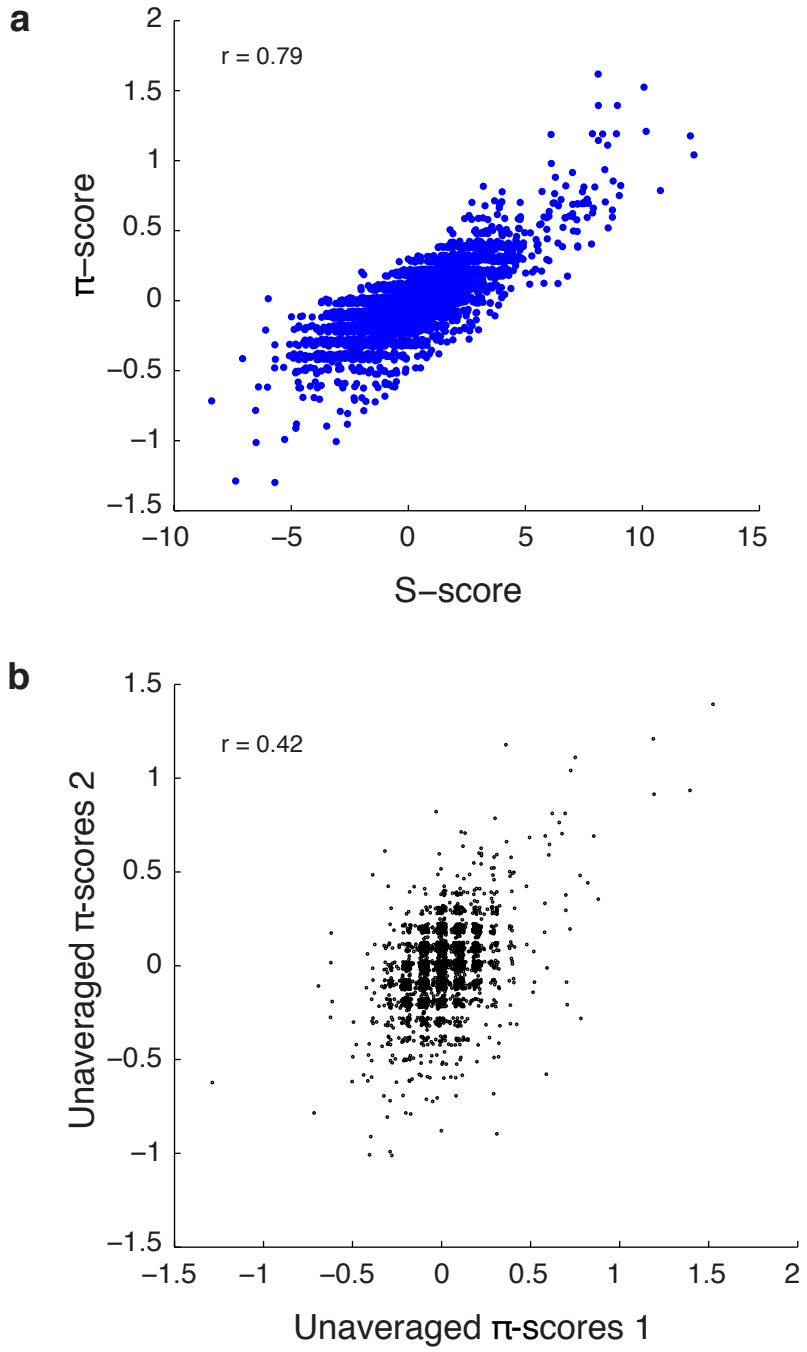

Comparison of GI scoring systems. (**a**) Comparison between the *S-score* (used in this study) and the π-score methodology used in a similar study in *D. melanogaster*. Both scoring protocols make similar assumptions about the sparseness of strong GIs. Raw data was scored using the *S-score* (horizontal axis) or π -score (vertical axis) and Pearson correlation shown. (**b**) Data reproducibility based on biological replicates using the π-score. Each point on the scatter plot represents a pair-wise GI measurement from 2 independent biological replicates.

Supplementary Figure 4 – Knock-down efficiencies in the presence of a second esiRNA targeting a different gene

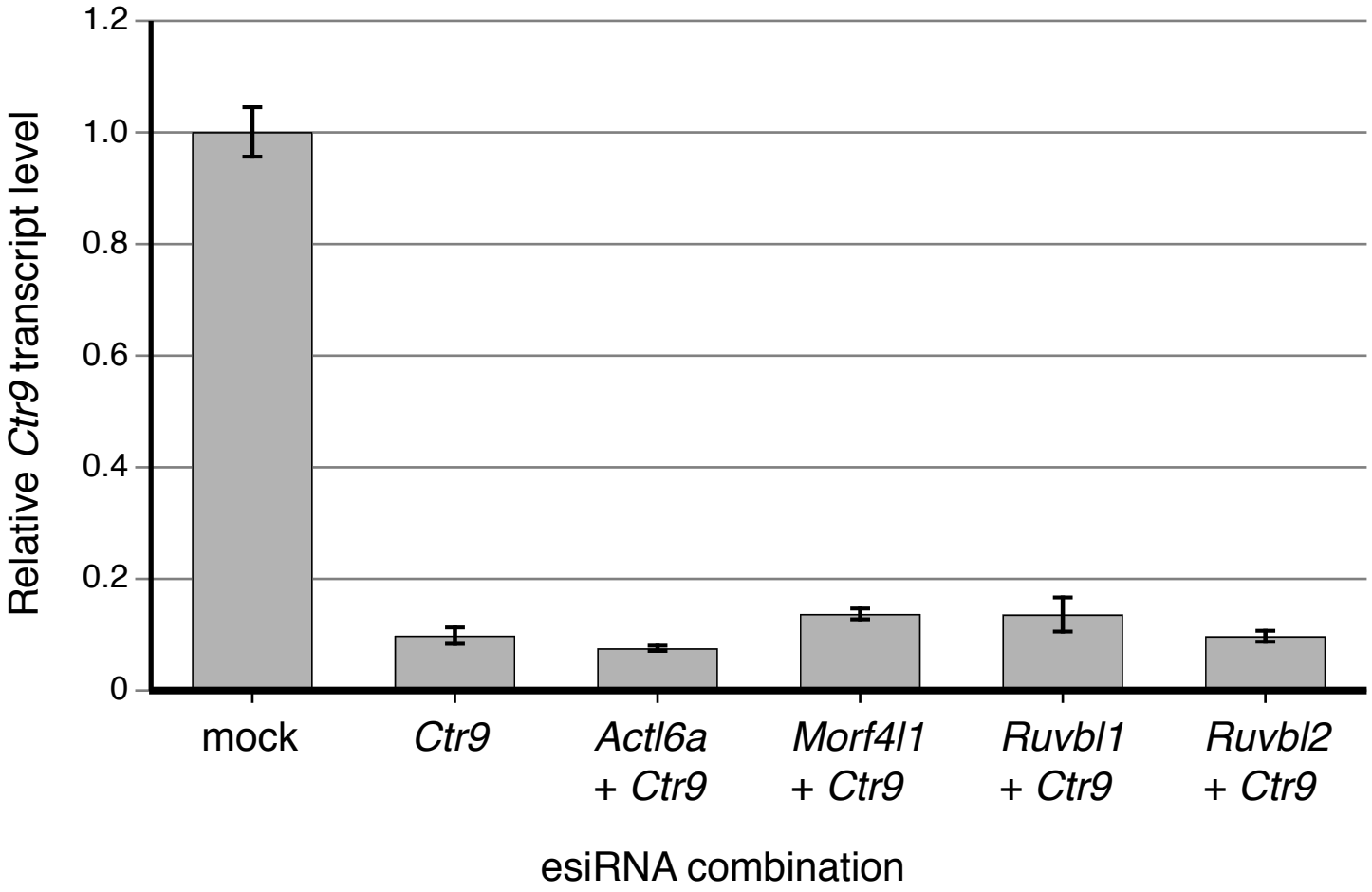

Knock-down efficiencies in the presence of a second esiRNA targeting a different gene. Cells were either mock-transfected, transfected only with Ctr9 esiRNA or a combination of esiRNA against Ctr9 and esiRNA against another gene. Ctr9 transcript levels were quantified by qRT-PCR and data presented is relative to the mock-transfected sample. Error bars represent standard deviation and are derived from four replicates (n = 4).

Nature Methods: doi:10.1038/nmeth.2398

Supplementary Figure 5 – Immunoblot analysis using two independent *Leo1* esiRNA designs.

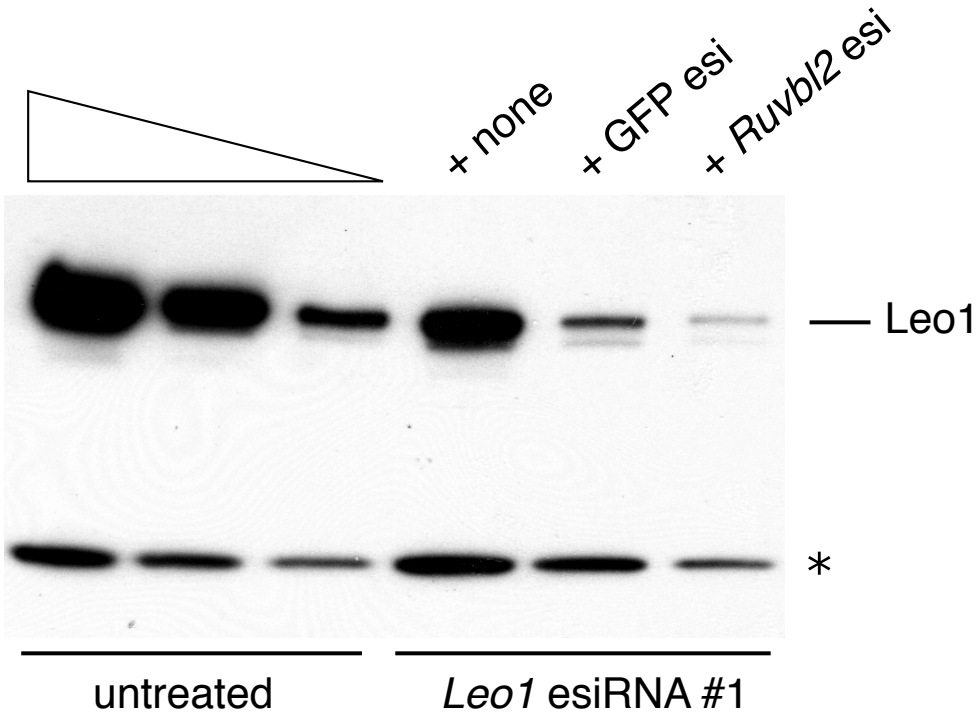

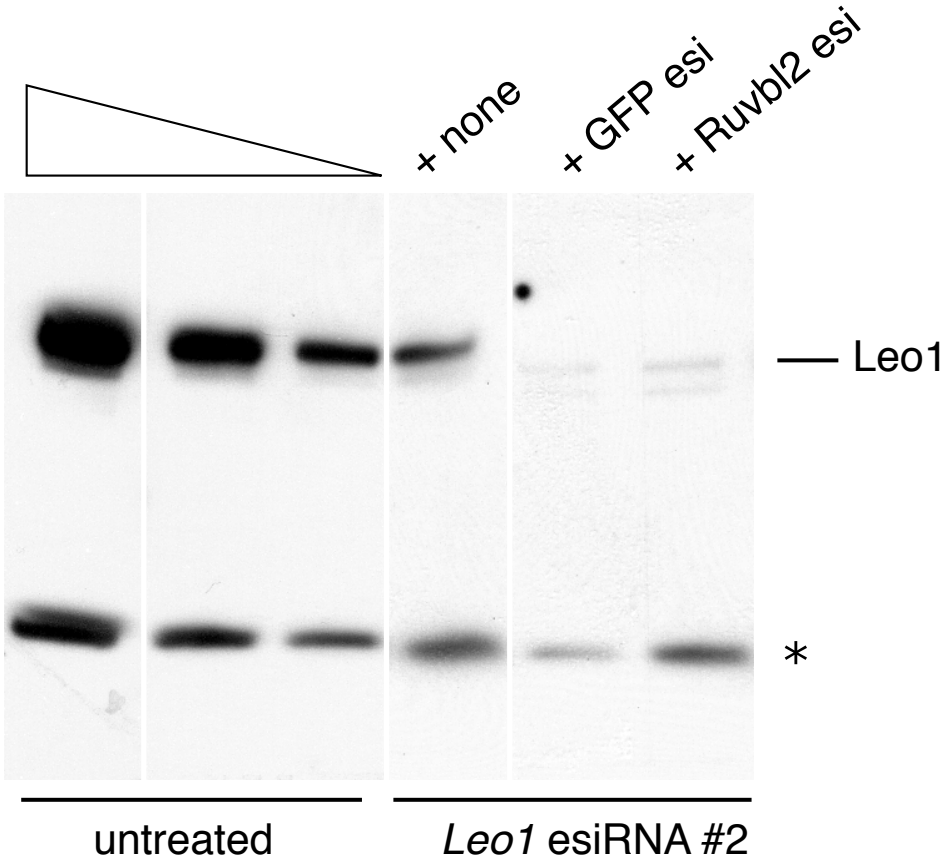

Immunoblot analysis using two independent *Leo1* esiRNA designs. Cells were harvested 72 hours post transfection. As *Leo1* depletion causes severe growth phenotype, equalizing protein concentration between samples proved to be difficult. Therefore different amounts of untreated cell extract were used (left part of the blots) and equivalent amounts of the total cell culture were loaded. Anti-Leo1 polyclonal antibody (Proteintech), detecting a 105 kDa band, was used. An unidentified cross-reacting band of approximately 30kD, marked by as '*', serves as a reference for protein levels in each lane.

Nature Methods: doi:10.1038/nmeth.2398

Supplementary Figure 6 – Cutoff definitions for positive and negative GIs

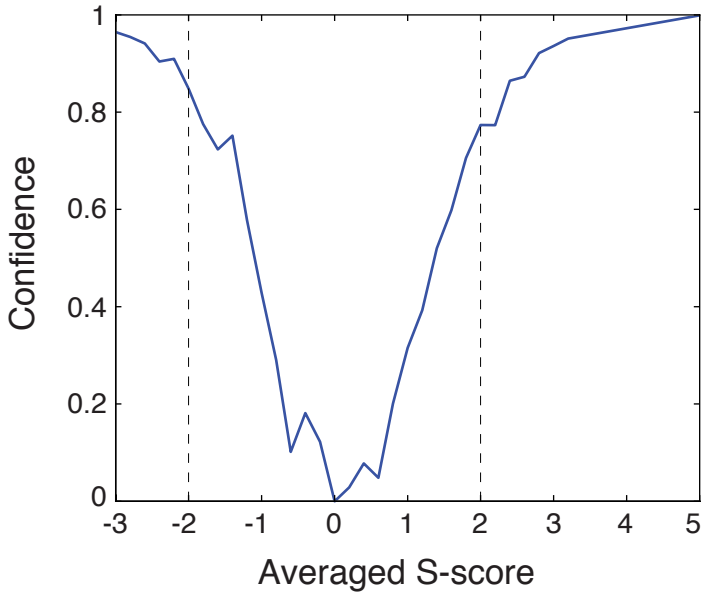

Cutoff definitions for positive and negative GIs. Cutoffs were defined at approximately 75% confidence that the observed interaction is real based on a confidence curve as in Collins et al, 2006.

Supplementary Figure 7 – GI scores derived from alternative esiRNA designs for the same gene are highly correlated

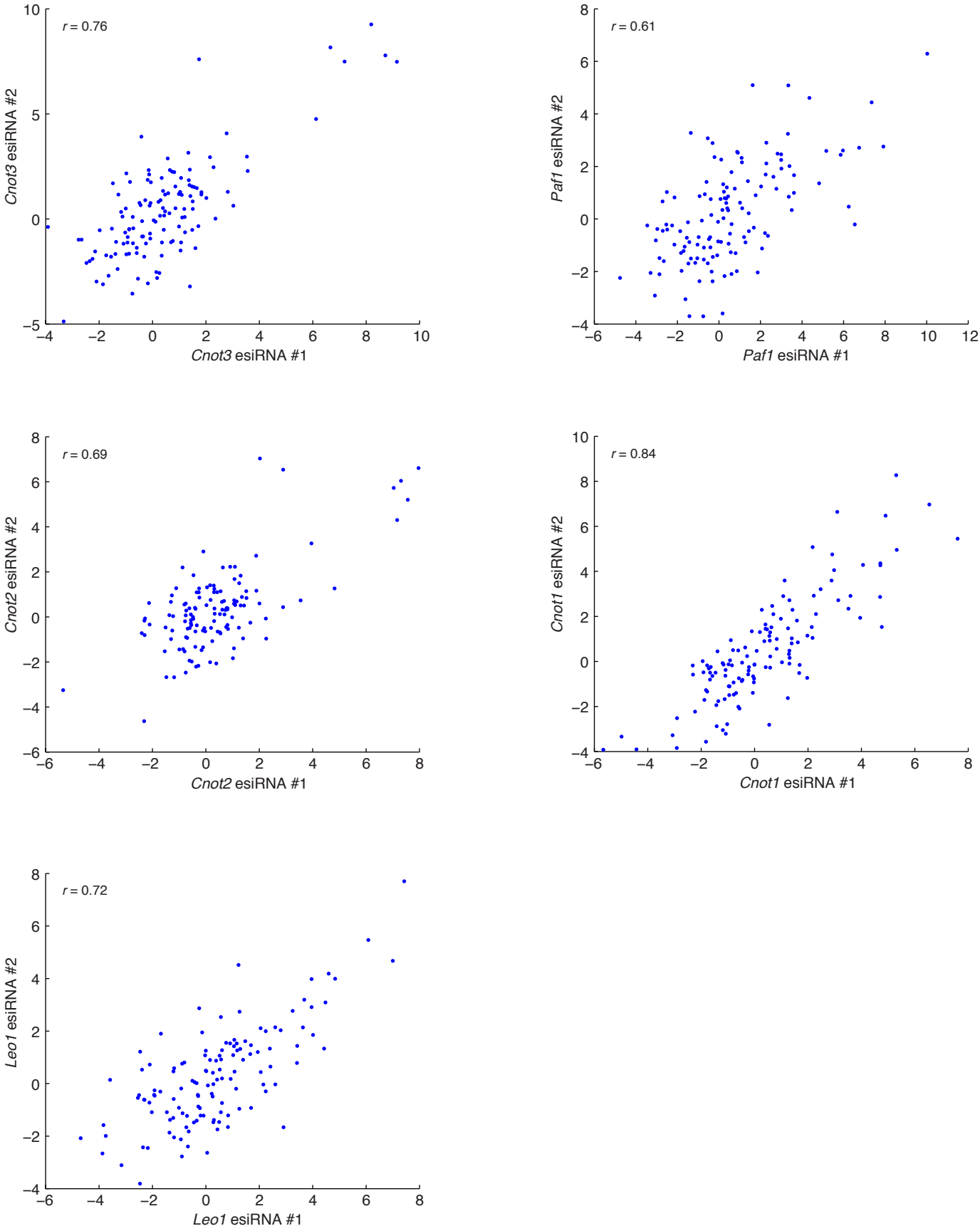

GI scores derived from alternative esiRNA designs for the same gene are highly correlated. For five genes, two alternative esiRNA designs targeting different parts of the transcript were used to generate GI profiles and these were plotted against each other. The values correspond to *S-scores* and the correlation coefficients were provided.

Nature Methods: doi:10.1038/nmeth.2398

Supplementary Figure 8 – Comparison of genetic data to HumanNet interactions

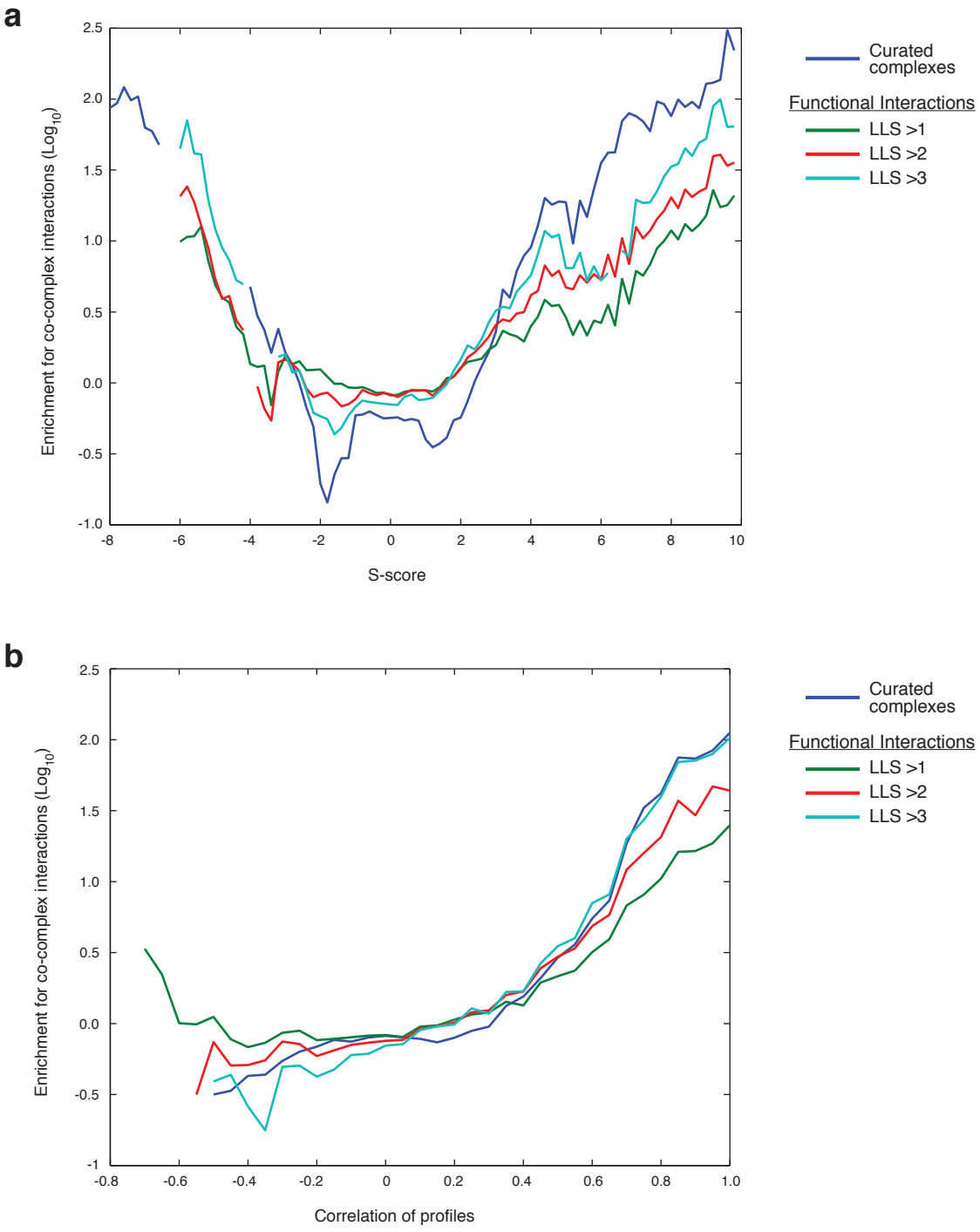

Comparison of genetic data to HumanNet interactions. (**a**) Correspondence of *S-scores* and (**b**) Pearson correlation of profiles on curated and unbiased functional interaction dataset called HumanNet at low (LLS > 1) to high (LLS > 3) stringency cutoffs. To compute the enrichment over random (*y*-axis), one first computes the fraction *f* of interactions at each score *x* that overlap with each dataset (bin size of 1.5). The enrichment is the ratio *f*/*r*, where *r* is the fraction of random protein pairs that overlap with each dataset.

Nature Methods: doi:10.1038/nmeth.2398

Supplementary Figure 9 – Synergistic effect of the PARP inhibitor ABT-888 and knock-down of Rtf1, a member of the PAF1 complex

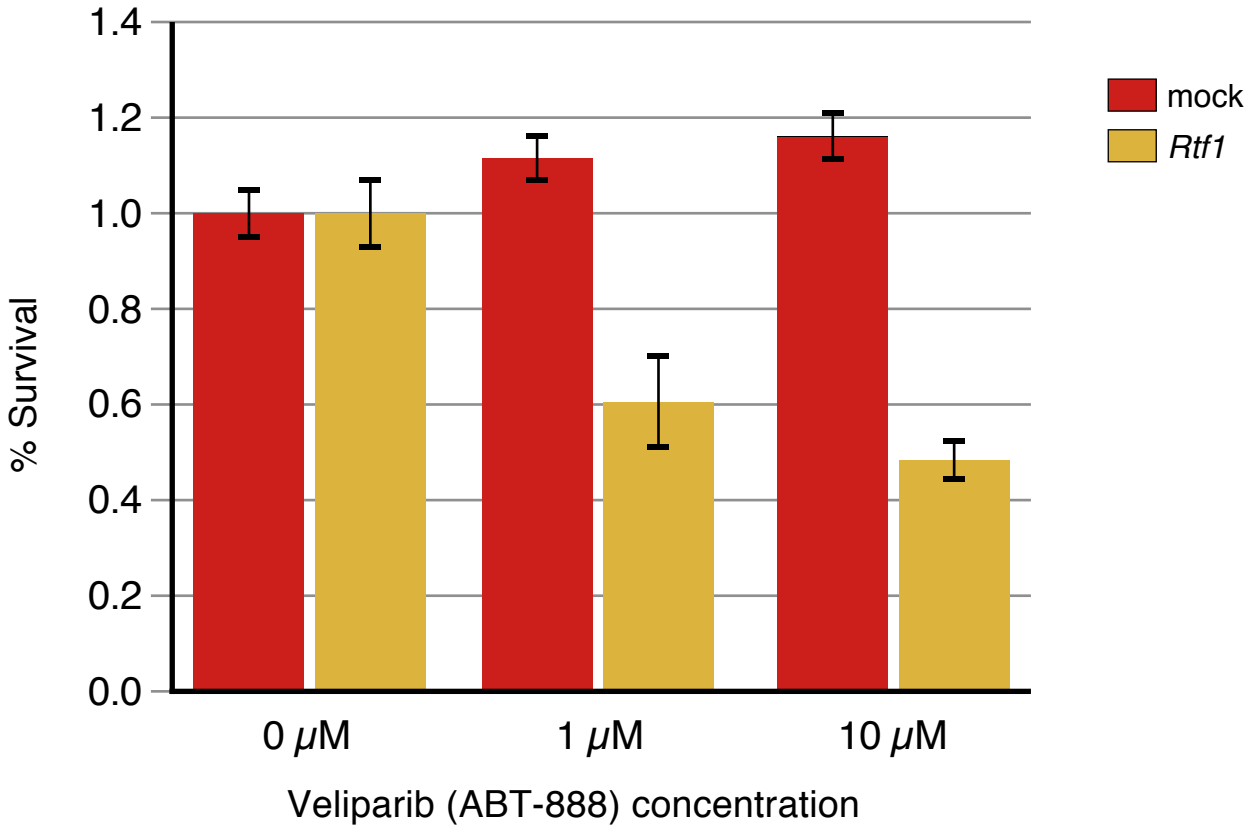

Synergistic effect of the PARP inhibitor ABT-888 and knock-down of *Rtf1*, a member of the PAF1 complex. Cells were either mock-transfected (mock) or transfected with *Rtf1* esiRNA. 24 hours post-transfection the cells were treated with ABT-888 at two different concentrations (1 and 10 μM). Cells were counted 72 hours post transfection. Data presented on the graph has been normalized to the respective mock cell counts. Error bars represent standard deviation and are derived from two replicates (n = 2).

Nature Methods: doi:10.1038/nmeth.2398

Supplementary Table 1

qPCR quantification of transcript levels after esiRNA knockdown.

gene#	% remaining transcript
Actl6a	0.9075192
Actl6b	0.1626677
Actr8	0.2268798
bard1	0.2044755
Bmi1	0.1008302
Brca1	1.7411011
Cbx3	0.1855654
Cbx4	0.5509526
Cbx5	0.3789291
cdc37	0.2300469
cdc73	0.3230882
Cnot1	0.0973956
Cnot2	0.5034778
cnot3	1.1250585
cnot4	0.3609823
cnot6	0.463294
cnot6l	0.2365144
cnot7	0.5823668
cnot8	0.4665165
Ddx17	0.1538931
Ddx5	0.1560413
Dmap1	0.2365144
Dnmt1	0.289172
Dnmt3a	0.1486509
Dnmt3b	0.208772
Dzip3	0.2206757
Eed	0.1755556
Elp3	0.0693481
Ep400	0.4204482
Epc1	1.0069556
Exosc1	0.1215819
Ezh2	0.1719427
H2afv	1.2397077
H2afz	0.0480273
Hcfc1	0.2284579
Hdac1	0.1241366
Ing1	1.9185282
Ino80	0.9930925
Jarid2	0.1907824
Kat2a	0.1830107
Leo1	0.1719427
Mbd2	3.0314331
Morf4l1	0.5987394
Morf4l2	0.0824692
Mta2	0.5212329
Mtf2	0.6328783
Mybbp1a	0.2030631
Myst1	0.2698071
Ncor2	0.4117955
Paf1	0.2660925
Parp1	0.07966
Parp2	0.2534899
Rbbp4	0.4117955
Rbbp7	0.3711309
Ring1	0.3584888
Rnf168	0.1695755
Rnf2	1.7900501
Rtf1	0.2606164
Ruvbl1	0.1051121
ruvbl2	0.3560125
Sap30l	0.5823668
Satb2	0.5743492
Sin3a	0.2044755
Sin3b	0.5703819
Sirt1	0.4475125
Smarca2	1.6817928
Smarca4	0.329877
Spop1	0.1649385
Ssrp1	0.2381595
Supt16h	0.3584888
Suv420h1	1.0424658
Suv420h2	1.0867349
Suz12	0.5321851
Tbl1x	0.2237563
Tbl1xr1	0.2284579
Tet1	0.5248583
Tet2	1.2834259
Trrap	0.5823668

Nature Methods: doi:10.1038/nmeth.2398

Supplementary Table 4

Manually curated functional modules and pathways list

module name	members								
INTEGRATOR	INTS2	INTS1	INTS8	INTS11	INTS4				
RBBP	RBBP7	RBBP4							
PAF	CDC73	SUPT16H	PAF1	LEO1	CTR9	RTF1			
PRC1	CBX4	BMI1	RING1	EZH2					
CNOT-core	CNOT3	CNOT2	CNOT1						
MORF	MORF4L2	MORF4L1							
DDX	DDX17	DDX5							
INO80	IES6	INO80	IES2						
COHESIN	SMC1A	SMC3	SMC1B						
RUVBL	RUVBL1	ACTL6A	RUVBL2						
ELONGATOR	ELP4	ELP3							
BRCA	BRCA1	BARD1							
PARP	PARP1	PARP2							
CONDENSIN	SMC2	SMC4							
CNOT-extension	CNOT8	CNOT7	CNOT6	CNOT4					
MCM	MCM7	MCM6	MCM4	MCM2					
MEDIATOR	MED21	MED11	MED12	MED1	MED6	MED7	MED4	MED9	MED13
UT	UTX	UTY							
P-TEFb	CCNT1	CDK9	ELL						
SIRT	SIRT1	TBL1X							
HDAC	HDAC1	HDAC2							
H2A	H2AFV	H2AFZ							

Nature Methods: doi:10.1038/nmeth.2398

Supplementary Table 5

Inter-module GI bundle P-values used in the module map in Figure 4.

Module1 <--> Module2	P-value	Genetic interaction sign (1 positive, -1 negative)
PAF <--> CNOT-core	0	1
PAF <--> INTEGRATOR	0.0083	1
SIRT <--> H2A	8.00E-04	-1
UTX <--> CNOT-core	0.0097	-1
CNOT-core <--> RUVBL	3.00E-04	1
PAF <--> UTX	3.00E-04	-1
H2A <--> RBBP	0.0049	1
DDX <--> RBBP	0.0096	1
MCM <--> RUVBL	0.0027	-1
MORF <--> PRC1	0.0048	-1
PAF <--> H2A	0	1
PAF <--> HDAC	0.0061	1
PAF <--> CONDENSIN	0	-1
PAF <--> RUVBL	0	1
MCM <--> PAF	0.0017	-1
PAF <--> PARP	2.00E-04	-1
MORF <--> PAF	3.00E-04	-1
COHESIN <--> INO80	0.0071	-1

Nature Methods: doi:10.1038/nmeth.2398